

Mechanistic Insight into the Formation of Acetic Acid from the Direct Conversion of Methane and Carbon Dioxide on Zinc-Modified H-ZSM-5 Zeolite

Jian-Feng Wu,[†] Si-Min Yu,[†] Wei David Wang,[†] Yan-Xin Fan,[†] Shi Bai,[†] Chuan-Wei Zhang,[‡] Qiang Gao,[‡] Jun Huang,^{||} and Wei Wang^{*,†}

[†]State Key Laboratory of Applied Organic Chemistry, College of Chemistry and Chemical Engineering, Lanzhou University, Lanzhou, Gansu 730000, P.R. China

[‡]National Engineering Research Center for Fine Petrochemical Intermediates, Lanzhou Institute of Chemical Physics, Chinese Academy of Sciences, Lanzhou, Gansu 730000, P.R. China

^{||}Laboratory for Catalysis Engineering, School of Chemical and Biomolecular Engineering, The University of Sydney, New South Wales 2006, Australia

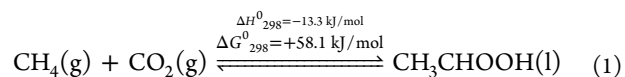
Supporting Information

ABSTRACT: Methane and carbon dioxide are known greenhouse gases, and the conversion of these two C₁-building blocks into useful fuels and chemicals is a subject of great importance. By solid-state NMR spectroscopy, we found that methane and carbon dioxide can be co-converted on a zinc-modified H-ZSM-5 zeolite (denoted as Zn/H-ZSM-5) to form acetic acid at a low temperature range of 523–773 K. Solid-state ¹³C and ¹H MAS NMR investigation indicates that the unique nature of the bifunctional Zn/H-ZSM-5 catalyst is responsible for this highly selective transformation. The zinc sites efficiently activate CH₄ to form zinc methyl species (–Zn–CH₃), the Zn–C bond of which is further subject to the CO₂ insertion to produce surface acetate species (–Zn–OOCCH₃). Moreover, the Brønsted acid sites play an important role for the final formation of acetic acid by the proton transfer to the surface acetate species. The results disclosed herein may offer the new possibility for the efficient activation and selective transformation of methane at low temperatures through the co-conversion strategy. Also, the mechanistic understanding of this process will help to the rational design of robust catalytic systems for the practical conversion of greenhouse gases into useful chemicals.



INTRODUCTION

With the increasing demands in new energies due to the global environmental concerns, co-conversion of methane and carbon dioxide into valuable products at mild conditions represents one of the most important subjects in C₁ chemistry.¹ Development of effective processes for such conversion has to deal with the challenging issue of the inherent stability of both CH₄ and CO₂: the C–H bond energy of CH₄ is 435 kJ/mol, and the standard enthalpy for CO₂ formation is –394 kJ/mol.^{1e,2} Hence, it is not surprising that the process for CO₂ reforming of CH₄ (indirect co-conversion) into syngas (CO and H₂) requires harsh reaction condition (*T* > 1000 K).^{1e} In contrast to the indirect approach, the direct co-conversion toward the formation of acetic acid (eq 1), albeit being thermodynamically unfavorable, is an atom-economic^{1e} process and may be operated under mild conditions.^{1c}



Indeed, the direct co-conversion of CH₄ and CO₂ into acetic acid or its equivalents having been examined not only theoretically,³ it has also been experimentally attempted under homogeneous,⁴ heterogeneous,⁵ gas-phase,⁶ and plasma⁷ conditions. For example, Huang et al.^{5b} reported the first example of using the Cu/Co-based metal oxide to achieve the co-conversion of CH₄ and CO₂ under heterogeneous conditions. Alcohols, aldehydes, ketones, carboxylic acids, and cyclopentane derivatives were observed as the reaction products and the maximum selectivity for acetic acid is 28%.^{5b} In each case, however, the product distribution is quite broad, and the reported yield of acetic acid from the direct conversion of CH₄ and CO₂ is very low.^{5c,e}

Meanwhile, limited by the experimental methods, little is known so far about the possible mechanisms for the direct conversion of CH₄ and CO₂ into acetic acid on solid catalysts. Huang et al.^{5b} proposed the possible formation of CH_{*x*} and CH_{*x*}O species on the Cu/Co-based metal oxide by the FTIR

Received: July 9, 2013

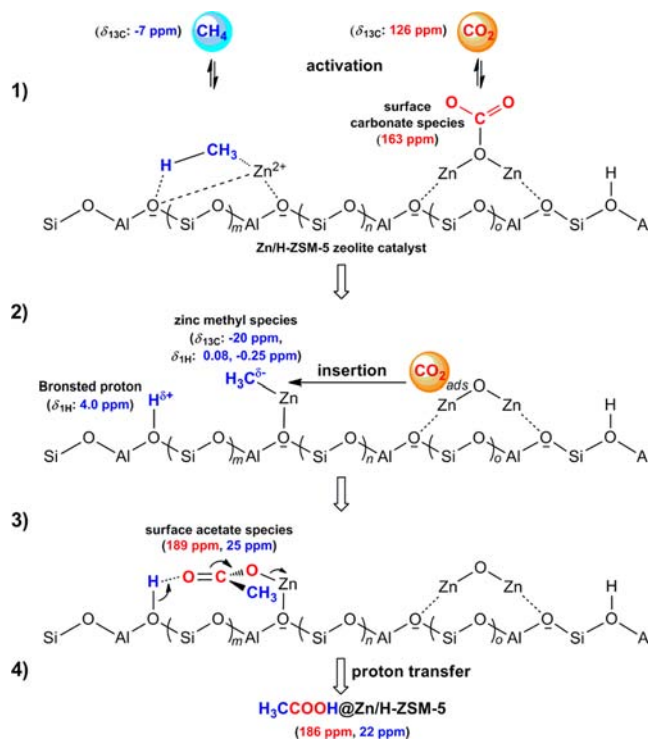
Published: August 27, 2013

measurement. Ding et al.^{5c} speculated that M–CH₃ species was mainly formed on Pd/SiO₂, while M–CH₂ and M–CH₃ species were produced on Rh/SiO₂. In addition, Ding et al.^{5c} and Wilcox et al.^{5c} suggested the formation of CH₃COO[−] species as the preliminary products by FTIR and DRIFT, respectively. However, the identification of the key intermediates is fragmentary or ambiguous so far. Thus, in addition to the poor selectivity and low yield, the convincing mechanism involved in the co-conversion of CH₄ and CO₂ has not been acknowledged and none of these investigations has been dealing with the zeolite systems.

Importantly, considerable progress on methane activation has been achieved on metal-exchanged zeolites.^{2d,8,9} Several research groups⁸ have found that zinc-modified ZSM-5 and BEA zeolites could activate methane under mild conditions. On the basis of the recent progress^{2d,8,9} in methane activation on bifunctional zeolites, we report herein the solid-state NMR investigation on a highly selective formation of acetic acid upon the co-conversion of CH₄ and CO₂ on a zinc-modified H–ZSM-5 zeolite (denoted as Zn/H–ZSM-5) at the relatively low temperature range of 523–773 K. By solid-state ¹³C and ¹H MAS NMR spectroscopy,¹⁰ the detailed reaction mechanism involved in this transformation has been revealed. Although this work is only a spectroscopic study on the working catalyst at the present stage, the information disclosed herein may stimulate the research toward the direct formation of acetic acid from methane and carbon dioxide on multifunctional solid catalysts. We also expect that our mechanistic understanding will shed light on the rational design of robust catalytic systems for practical conversion of greenhouse gases.

In this contribution, we explored the new possibility for efficient activation and selective transformation of methane through the co-conversion strategy. By solid-state NMR spectroscopy, we found that acetic acid could be selectively formed as the sole product via the reaction of CH₄ and CO₂ on a bifunctional Zn/H–ZSM-5 zeolite at temperatures higher than 523 K. We identified, by solid-state ¹³C MAS NMR spectroscopy, the formation of zinc methyl species (–Zn–CH₃) and carbonate species as the primary surface intermediates upon the activation of CH₄ and CO₂, respectively. Selective ¹³C-labeling experiments clarified that the formation of acetic acid indeed follows the co-conversion pathway: the methyl group of acetic acid originates from methane and the carbonyl group from carbon dioxide. On the basis of these observations, we proposed the co-conversion mechanism of CH₄ and CO₂ on Zn/H–ZSM-5 zeolite (Scheme 1), which includes three key steps: (i) the simultaneous formation of zinc methyl species and Brønsted proton via methane activation, (ii) the insertion of CO₂ into the Zn–C bond of surface zinc methyl species to produce surface acetate species (–Zn–OOCCH₃) as a key intermediate, and (iii) the final formation of acetic acid via the proton abstraction from Brønsted acid sites to surface acetate species. We performed additional experiments to verify the following issues which are critical to the mechanism proposed herein: (i) ¹H MAS NMR experiments confirmed that the Brønsted protons were formed on the working catalyst during methane activation; (ii) the reaction of CO₂ with deliberately isolated zinc methyl species confirmed the insertion of CO₂ into the Zn–C bond of zinc methyl species and the formation of surface acetate species; and (iii) the surface acetate species can abstract protons from the Brønsted acid sites to produce acetic acid in the reaction of Zn(CH₃COO)₂ with acidic H–ZSM-5 zeolite.

Scheme 1. Proposed Mechanism for the Co-Conversion of Methane and Carbon Dioxide into Acetic Acid on the Bifunctional Zn/H–ZSM-5 Zeolite^a



^a(Steps 1 to 2): CH₄ (blue) activation leads to the formation of zinc methyl species (–Zn–CH₃) and a Brønsted proton, while CO₂ (red) activation results in the formation of surface carbonate species. (Steps 2 to 3): insertion of CO₂ into zinc methyl species produces surface acetate species (–Zn–OOCCH₃) as a key intermediate. (Steps 3 to 4): surface acetate species abstracts the Brønsted proton to release acetic acid and to restore the Zn/H–ZSM-5 catalyst.

RESULTS

Co-conversion of Methane and Carbon Dioxide into Acetic Acid on Zn/H–ZSM-5 Zeolite.

The co-conversion of methane and carbon dioxide was conducted on Zn/H–ZSM-5 zeolite. The detailed procedures for the catalyst preparation¹¹ can be found in the literature (see Supporting Information [SI] for details). The synthesized Zn/H–ZSM-5 zeolite was thoroughly characterized by spectroscopic measurements, and the obtained results are in excellent agreement with those reported previously.¹¹ The reaction of ¹³C-labeled ¹³CH₄ and ¹³CO₂ on Zn/H–ZSM-5 zeolite was thus monitored by the ¹³C cross-polarization magic-angle-spinning (CP/MAS) NMR spectroscopy, and the obtained results are shown in Figure 1.

When the reaction was carried out at 473 K (Figure 1a), zinc methyl species (–Zn–¹³CH₃)^{8b,d} appeared at –20 ppm and surface carbonate species¹² appeared at 163 ppm, indicating the activation of ¹³CH₄ and ¹³CO₂ on the catalyst, respectively (vide infra). The formation of acetic acid starts at ~523 K (Figure 1b), evidenced by the ¹³C NMR signals^{8d,g,13} coexisting at 22 ppm (methyl group) and 186 ppm (carbonyl group). The signal intensity of zinc methyl species (–Zn–¹³CH₃, at –20 ppm) decreased after the formation of acetic acid at 573 K (Figure 1c) and disappeared at 673–773 K (spectra d and e of Figure 1), implying the further transformation of zinc methyl species to acetic acid. Meanwhile, the signal intensities of acetic acid (at 22 and 186 ppm) slightly increased at 573 K (Figure

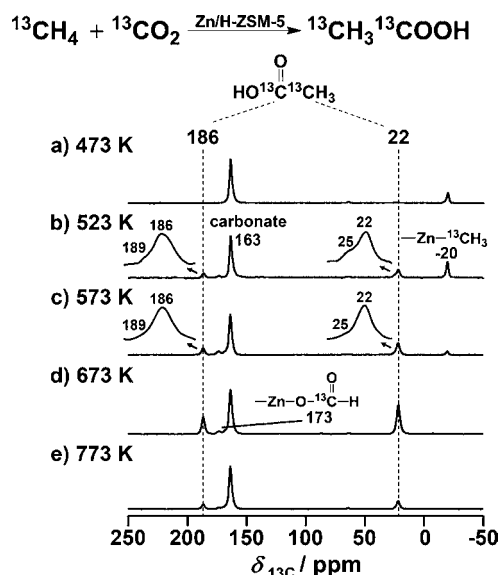


Figure 1. Solid-state NMR investigation into the reaction of methane and carbon dioxide over Zn/H-ZSM-5 zeolite. The ^{13}C CP/MAS NMR spectra were recorded upon the reaction of $^{13}\text{CH}_4$ and $^{13}\text{CO}_2$ on Zn/H-ZSM-5 zeolite at (a) 473 K, (b) 523 K, (c) 573 K, (d) 673 K, and (e) 773 K. The spectra were recorded with a 4 mm NMR probe.

1c) and reached the maximum around 673 K (Figure 1d) but decreased at 773 K (Figure 1e). The decreased signal of acetic acid indicates the decomposition of acetic acid back to $^{13}\text{CH}_4$ and $^{13}\text{CO}_2$ at high temperature.¹³ The occurrence of this reverse decomposition was confirmed by the reaction of acetic acid on Zn/H-ZSM-5 zeolite (Figure S5 in the SI). Thus, the optimum temperature for the selective formation of acetic acid is around 673 K (Figure 1d). In addition, we found the subtle formation of surface acetate species¹³ ($-\text{Zn}-\text{OO}^{13}\text{C}^{13}\text{CH}_3$ at 25 and 189 ppm, the enlargement in spectra b and c of Figure 1) and surface formate species^{8d} (at 173 ppm, spectra b–e of Figure 1) on the working catalyst. The formation of these surface intermediates would provide additional evidence for the reaction mechanism (vide infra). Similar information was also obtained from the corresponding ^{13}C high-power proton decoupling (HPDEC) MAS NMR spectra (Figure S6 in the SI). The ^{13}C HPDEC MAS NMR investigation on the sealed glass samples (see Experimental Section in the SI) gave the identical results (Figure S7 in the SI). All these data verified the selective formation of acetic acid via the reaction of CH_4 and CO_2 on Zn/H-ZSM-5 zeolite at the temperature range of 523–773 K.

In order to trace the origin of the carbon atoms on the formed acetic acid, we alternated the ^{13}C -labeling for either CH_4 or CO_2 and conducted the reaction under the above-applied conditions. The resulting ^{13}C CP/MAS NMR spectra are shown in Figure 2. Methane ($^{13}\text{CH}_4$) activation was observed at 473 K before the formation of acetic acid (Figure 2a, left), as evidenced by the dominating signal at -20 ppm for zinc methyl species ($-\text{Zn}-^{13}\text{CH}_3$). The activation of carbon dioxide ($^{13}\text{CO}_2$) on Zn/H-ZSM-5 zeolite was also observed at this temperature, as evidenced by the formation of surface carbonate species at 163 ppm¹² (Figure 2a, right). When the reactions occurred at 523 K or above, the formation of acetic acid could be identified, depending on the position of ^{13}C labeling, by either the signal at 22 ppm for the methyl group (Figure 2b to 2e, left) or the signal at 186 ppm for the carbonyl

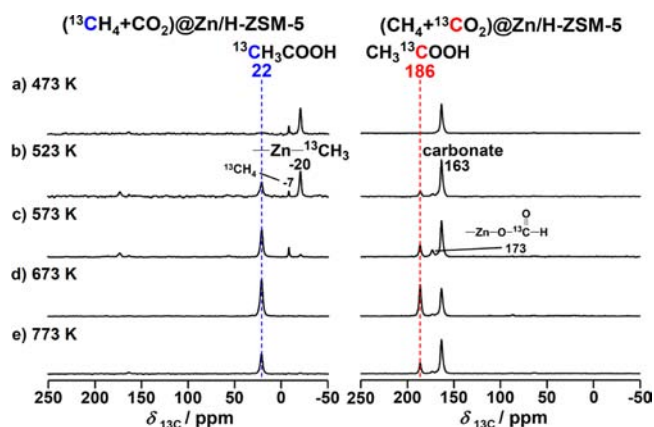


Figure 2. Solid-state NMR investigation into the origin of the carbon atoms on acetic acid. The ^{13}C CP/MAS NMR spectra were recorded upon the reactions of ^{13}C -enriched methane ($^{13}\text{CH}_4$) with nonlabeled carbon dioxide (CO_2) (left) and of nonlabeled methane (CH_4) with ^{13}C -enriched carbon dioxide ($^{13}\text{CO}_2$) (right) on Zn/H-ZSM-5 zeolite at (a) 473 K, (b) 523 K, (c) 573 K, (d) 673 K, and (e) 773 K. The signal at 173 ppm comes from surface formate species, the formation of which can be attributed to the oxidation of surface methoxy species ($-\text{Zn}-\text{O}-\text{CH}_3$).^{8d} The spectra were recorded with a 4 mm NMR probe.

group of acetic acid (Figure 2b to 2e, right). Therefore, it can be concluded that the formation of acetic acid is indeed due to the co-conversion of CH_4 and CO_2 : the methyl group of acetic acid originates from methane and the carbonyl group from carbon dioxide. Similar information was obtained from the corresponding ^{13}C HPDEC MAS NMR spectra (Figure S8 in the SI). The labeling experiments thus offered clear evidence for the origin of the carbon atoms on acetic acid, based on which the reaction mechanism can be proposed (vide infra).

Mechanism for the Co-conversion of Methane and Carbon Dioxide. On the basis of the above results, we proposed a mechanism for the formation of acetic acid via the co-conversion of CH_4 and CO_2 on Zn/H-ZSM-5 zeolite (Scheme 1). First, CO_2 activation on Zn/H-ZSM-5 zeolite produces a surface carbonate species (^{13}C NMR chemical shift of 163 ppm, see (Step 1)). Meanwhile, methane activation forms a zinc methyl species ($-\text{Zn}-\text{CH}_3$, ^{13}C NMR chemical shift of -20 ppm) and a Brønsted proton (Step 1 to Step 2). The activated CO_2 then inserts into the Zn–C bond of zinc methyl species to produce the surface acetate species ($-\text{Zn}-\text{OOCCH}_3$, ^{13}C NMR chemical shift of 25 and 189 ppm) as a key intermediate (Step 2 to Step 3). The latter further abstracts protons from the Brønsted acid site to form acetic acid (^{13}C NMR chemical shift of 22 and 186 ppm) as the final product (Step 3 to Step 4). To validate the mechanism proposed in Scheme 1, three key issues should be further addressed. The first is the formation of the zinc methyl species ($-\text{Zn}-\text{CH}_3$) and the Brønsted proton by methane activation on Zn/H-ZSM-5 zeolite. The second is the insertion of CO_2 into the Zn–C bond of $-\text{Zn}-\text{CH}_3$ surface species to produce surface acetate species ($-\text{Zn}-\text{OOCCH}_3$). The third is the formation of acetic acid via the proton abstraction from Brønsted acid sites to surface acetate species ($-\text{Zn}-\text{OOCCH}_3$). Accordingly, we performed further experiments to verify these issues.

Activation of Methane. By solid-state ^{13}C MAS NMR spectroscopy, we have observed the formation of zinc methyl species ($-\text{Zn}-^{13}\text{CH}_3$) starting from 473 K (spectrum a of Figure 1 and spectrum a of Figure 2, left), which implies the

activation of methane ($^{13}\text{CH}_4$) through the dissociative adsorption^{8a-c} mechanism (Scheme 1, Step 1 to Step 2). Similar information for methane activation on a Zn–ZSM-5 zeolite (without Brønsted acid sites) has been proposed by Kazansky et al. on the basis of the diffuse reflectance infrared Fourier transform (DRIFT) study.^{8a} Meanwhile, this mechanism was further supported by Ivanova and co-workers, who observed the zinc methyl species by ^{13}C MAS NMR spectroscopy.^{8b,c} In order to offer the mechanistic insight into this step, we further confirmed the simultaneous formation of the Brønsted proton upon the activation of ^{13}C -labeled methane on Zn/H–ZSM-5 zeolite by ^1H MAS NMR spectroscopy. As shown in Figure 3, dotted line, the ^1H MAS

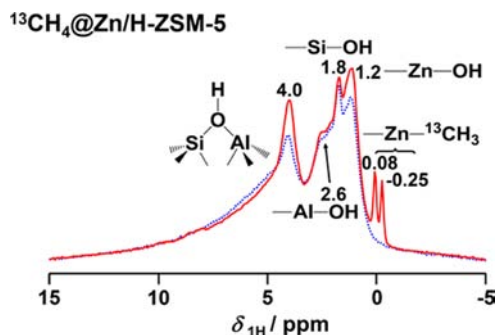


Figure 3. Experimental evidence for the formation of Brønsted protons: ^1H MAS NMR spectra of the fresh Zn/H–ZSM-5 zeolite (dotted line) and the Zn/H–ZSM-5 working catalyst upon the activation of $^{13}\text{CH}_4$ (51 mbar) at 453 K for 45 min (solid line, unreacted $^{13}\text{CH}_4$ was removed upon evacuation). The ^1H doublet peaks at 0.08 and -0.25 ppm with $J_{\text{H}-^{13}\text{C}} = 132$ Hz confirmed the formation of zinc methyl species ($-\text{Zn}-^{13}\text{CH}_3$) and the increased signal at 4.0 ppm identified the simultaneous formation of the Brønsted proton upon dissociative adsorption of CH_4 , as shown in Scheme 1, Step 1 to Step 2). The increased signal of $-\text{Zn}-\text{OH}$ groups at 1.2 ppm implies the dissociative adsorption of CH_4 on ZnO inside the Zn/H–ZSM-5 zeolite channels.^{8c} The spectra were recorded with a 4 mm NMR probe.

NMR signals for the fresh Zn/H–ZSM-5 zeolite at 4.0, 2.6, 1.8, and 1.2 ppm can be assigned to the protons of Brønsted acid sites, $-\text{Al}-\text{OH}$, $-\text{Si}-\text{OH}$, and $-\text{Zn}-\text{OH}$ groups, respectively.^{8g} After the reaction of $^{13}\text{CH}_4$ at 453 K for 45 min followed by the removal of unreacted $^{13}\text{CH}_4$ upon evacuation (no $^{13}\text{CH}_4$ signal exists in the corresponding ^{13}C HPDEC MAS NMR spectrum, see Figure S9 in the SI for details), ^1H doublet peaks appeared at 0.08 and -0.25 ppm with a separation of 132 Hz (Figure 3, solid line). These ^1H doublets are assigned to the protons of zinc methyl species ($-\text{Zn}-^{13}\text{CH}_3$), subjected to the $^1\text{H}-^{13}\text{C}$ scalar coupling¹⁴ with $J_{\text{H}-^{13}\text{C}} = 132$ Hz. Evidently, only a singlet at -0.08 ppm could be observed for the zinc methyl species ($-\text{Zn}-\text{CH}_3$) when ^{13}C -nonlabeled CH_4 was used (Figure S10 in the SI). Meanwhile, upon the formation of zinc methyl species ($-\text{Zn}-^{13}\text{CH}_3$), the ^1H signal intensity of Brønsted proton at 4.0 ppm was increased (Figure 3), indicating the formation of additional Brønsted protons via the dissociative adsorption of $^{13}\text{CH}_4$ on Zn/H–ZSM-5 catalyst (Scheme 1, Step 1 to Step 2). Integration analysis of the difference spectrum according to Figure 3 showed that the ratio of the intensity increase at 0.08 and -0.25 ppm to that at 4.0 ppm is about 3.2 ± 0.2 . This result further confirmed the simultaneous formation of Brønsted proton and surface $-\text{Zn}-\text{CH}_3$ species (with the theoretical ratio of 1:3 for the ^1H atoms)

upon dissociative adsorption of CH_4 on Zn/H–ZSM-5 zeolite. Thus, upon the evacuation of unreacted methane, we were able to identify the ^1H chemical shifts for the zinc methyl species and the formation of the Brønsted proton by ^1H MAS NMR spectroscopy.

Insertion of Carbon Dioxide. Another aspect to validate the proposed mechanism is the insertion of CO_2 into the Zn–C bond of zinc methyl species ($-\text{Zn}-\text{CH}_3$) and the formation of surface acetate species as the key intermediate. Accordingly, upon the evacuation of unreacted $^{13}\text{CH}_4$, we isolated the zinc methyl species and studied its reactivity in the presence of $^{13}\text{CO}_2$ (Figure 4). As shown in Figure 4a, the exclusive signal at

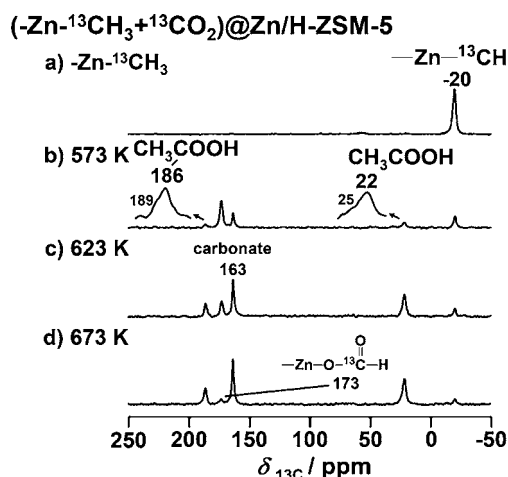


Figure 4. Solid-state NMR investigation on the CO_2 insertion into the Zn–C bond of zinc methyl species. ^{13}C CP/MAS NMR spectra were recorded for: (a) the isolated ^{13}C -enriched zinc methyl species ($-\text{Zn}-^{13}\text{CH}_3$); and upon the reaction of zinc methyl species ($-\text{Zn}-^{13}\text{CH}_3$) with 1 mbar of $^{13}\text{CO}_2$ at (b) 573 K, (c) 623 K, and (d) 673 K for 20 min on Zn/H–ZSM-5 catalyst. The signal at 173 ppm comes from surface formate species, the formation of which can be attributed to the oxidation of surface methoxy species ($-\text{Zn}-\text{O}-\text{CH}_3$).^{8d} The spectra were recorded with a 4 mm NMR probe.

-20 ppm indicates the successful isolation of the zinc methyl species ($-\text{Zn}-^{13}\text{CH}_3$).^{8b,f} Upon the reaction of zinc methyl species with $^{13}\text{CO}_2$ at 573, 623, and 673 K (spectra b to d of Figure 4), the formation of acetic acid is evidenced by the ^{13}C NMR signals at 22 ppm (methyl group) and 186 ppm (carbonyl group).^{8f,g,13} The signal intensity of zinc methyl species ($-\text{Zn}-^{13}\text{CH}_3$, at -20 ppm) decreased after the formation of acetic acid (spectra b to d of Figure 4), indicating the involvement of zinc methyl species in the formation of acetic acid. In addition, we found a tiny amount of surface acetate species¹³ ($-\text{Zn}-\text{OO}^{13}\text{C}^{13}\text{CH}_3$ at 25 and 189 ppm (the enlargement in Figure 4b) formed at 573 K, confirming its role as the key intermediate during the formation of acetic acid.

The high reactivity of zinc methyl species on Zn/H–ZSM-5 zeolite can be well understood in analogy to those of organozinc compounds in organometallic chemistry.¹⁵ Specifically, Ochiai et al. disclosed the direct synthesis of various carboxylic acids from the corresponding alkylzinc reagents and CO_2 .¹⁶ Kobayashi and Kondo developed an efficient process for the carboxylation of functionalized organozinc reagents with CO_2 in the presence of LiCl .¹⁷ Moreover, Knochel and co-workers reported that MgCl_2 -accelerated addition of functionalized organozinc reagents to CO_2 could yield the corresponding carboxylic acids.¹⁸ In all these cases, CO_2 insertion into the

Zn–C bond of organozinc reagents is common and essential. By ^{13}C solid-state NMR spectroscopy, we confirmed in this contribution that the CO_2 insertion to zinc methyl species could occur at temperatures of 573–673 K on Zn/H–ZSM-5 catalyst.

Proton Abstraction. The remaining issue for validation of the proposed mechanism is the formation of acetic acid via abstraction of protons from Brønsted acid sites to surface acetate species. Accordingly, we investigated the transformation of zinc acetate $[\text{Zn}(\text{CH}_3\text{COO})_2]$ on acidic H–ZSM-5 zeolite as a model reaction for proton abstraction from Brønsted acid sites (Figure 5). Figure 5a shows the ^1H MAS NMR spectrum

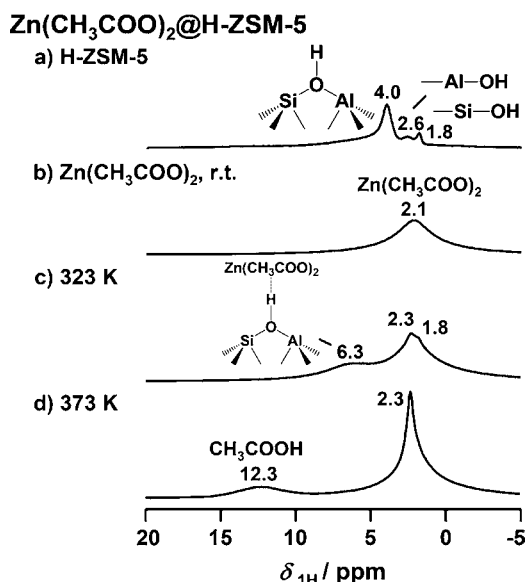


Figure 5. Solid-state NMR investigation on the formation of acetic acid via proton abstraction from the Brønsted acid sites to zinc acetate $[\text{Zn}(\text{CH}_3\text{COO})_2]$. The ^1H MAS NMR spectra were recorded for: (a) the activated H–ZSM-5 zeolite and (b) anhydrous zinc acetate $[\text{Zn}(\text{CH}_3\text{COO})_2]$, and upon the reaction of $\text{Zn}(\text{CH}_3\text{COO})_2$ on H–ZSM-5 zeolite at (c) 323 K and (d) 373 K for 20 min. The spectra were recorded with a 4 mm NMR probe.

of the activated H–ZSM-5 zeolite. The ^1H NMR signals at 4.0, 2.6, and 1.8 ppm are assigned to the protons of the Brønsted acid sites, $-\text{Al}-\text{OH}$, and $-\text{Si}-\text{OH}$ groups, respectively.¹⁹ The anhydrous zinc acetate $[\text{Zn}(\text{CH}_3\text{COO})_2]$ showed a broad signal centered at 2.1 ppm (Figure 5b), which can be assigned to the methyl groups. When H–ZSM-5 zeolite loaded with $\text{Zn}(\text{CH}_3\text{COO})_2$ was heated at 323 K for 20 min, a new broad ^1H resonance appeared at 6.3 ppm (Figure 5c), which could be due to the interaction (a similar interaction was described in the literature¹⁹) between Brønsted acid sites and $\text{Zn}(\text{CH}_3\text{COO})_2$. Upon heating the parallel sample at 373 K for 20 min (Figure 5d), the resonance at 6.3 ppm (Figure 5c) disappeared, and a broad signal was found at 12.3 ppm which was assigned to the proton²⁰ of carboxyl group in acetic acid. This result demonstrated that the abstraction of a proton from Brønsted acid sites to zinc acetate could be easily realized on H–ZSM-5 zeolite at a temperature higher than 373 K. Accordingly, it is very likely that the formation of acetic acid on Zn/H–ZSM-5 zeolite could be achieved via the abstraction of proton from Brønsted acid sites to surface acetate species at temperatures higher than 373 K.

DISCUSSION

The simultaneous transformation of CH_4 and CO_2 , both of which are greenhouse gases, is of multi-importance. Besides the essential need for methane conversion, utilization of carbon dioxide as a feedstock in chemical synthesis is also highly desirable. Albeit being a thermodynamically unfavorable reaction, the direct formation of acetic acid from CH_4 and CO_2 has an atom economy of 100% and, therefore, should deserve more research attention. We report herein the first example for the co-conversion of CH_4 and CO_2 on a bifunctional zeolite catalyst which affords acetic acid as the sole product.

We infer that the high selectivity for acetic acid should be attributed to the unique nature of the bifunctional catalyst (Scheme 1): (i) The bifunctional zeolite catalyst is very efficient and highly selective in activating CH_4 and CO_2 at low temperatures. Unlike in other cases in which a variety of $\text{M}-\text{CH}_x$ or $\text{M}-\text{OCH}_x$ surface species were proposed,^{5b} zinc methyl species ($-\text{Zn}-\text{CH}_3$) are selectively formed from methane activation on Zn/H–ZSM-5 zeolite. (ii) Zinc methyl species can effectively react with carbon dioxide through the insertion mechanism that has well been established in organometallic chemistry in homogeneous media. The surface carbonate species may serve as a reservoir for carbon dioxide to be inserted into the Zn–C bond of zinc methyl species. (iii) Most uniquely, unlike in other cases in which H_2^{Se} or $\text{H}\bullet$ ²¹ was proposed as an intermediate, the Brønsted proton formed from methane activation (see Figure 3) plays an important role in the final formation of acetic acid through proton transfer. The zeolite framework offers an excellent platform for stabilizing and transferring these Brønsted protons. Moreover, the acid strength of the Brønsted protons on Zn/H–ZSM-5 zeolite is strong enough to protonate the surface acetate species to form acetic acid.

Although the information disclosed herein is based on the spectroscopic investigation only, the mechanistic understanding may be of benefit to exploit the robust catalytic systems for practical co-conversion of CH_4 and CO_2 into industrial chemicals. For example, the co-conversion approach could be further optimized by using supercritical carbon dioxide²² (higher pressure as a key parameter), adding amines or alcohols²³ for further transformation (thermodynamic issue), and adjusting the zeolite topology, Si to Al ratio, as well as the metal types (activation energy issue).

CONCLUSION

We report herein the highly selective transformation of CH_4 and CO_2 into acetic acid on a zinc-modified Zn/H–ZSM-5 zeolite at the temperature range of 523–773 K. Solid-state NMR investigation reveals that, in difference from the previous proposals for other solid catalysts,⁵ the unique nature of the bifunctional Zn/H–ZSM-5 zeolite catalyst is responsible for the selective formation of acetic acid on Zn/H–ZSM-5 catalyst: the zinc sites efficiently activate CH_4 to selectively form zinc methyl species ($-\text{Zn}-\text{CH}_3$), the Zn–C bond of which is further subject to CO_2 insertion. Moreover, the Brønsted acid sites play an important role in the final formation of acetic acid via proton transfer. Our results demonstrate a viable method of efficient activation and selective transformation of methane at low temperatures through a co-conversion strategy. We expect that our approach will stimulate further research in the direct formation of acetic acid from methane and carbon dioxide on

multifunctional solid catalysts and that our mechanistic understanding of this process (Scheme 1) will provide insights into the rational design of robust catalytic systems for practical conversion of greenhouse gases into industrial chemicals. Research on the catalytic reaction test is now being conducted in this laboratory to address these issues.

■ ASSOCIATED CONTENT

■ Supporting Information

Detailed experimental procedures, characterization data (PXRD pattern and ^1H , ^{27}Al , and ^{29}Si solid-state NMR spectra) for the prepared Zn/H-ZSM-5 zeolite, solid-state NMR results for the decomposition of acetic acid, sealed glass insert experiment, adsorption and coadsorption (CH_4 , $^{13}\text{CH}_4$ + $^{13}\text{CO}_2$, CH_4 + $^{13}\text{CO}_2$, and $^{13}\text{CH}_4$ + CO_2). This material is available free of charge via the Internet at <http://pubs.acs.org>.

■ AUTHOR INFORMATION

Corresponding Author

wang_wei@lzu.edu.cn

Notes

The authors declare no competing financial interest.

■ ACKNOWLEDGMENTS

This work was financially supported by the National Natural Science Foundation of China (No. 20933009) and the 111 Project. We thank Profs. Jian-Tai Ma and Rong Li (Lanzhou University), and Mr. Xin-Hu Wu (Lanzhou Institute of Chemical Physics) for helpful discussion.

■ REFERENCES

- (1) (a) Crabtree, R. H. *Chem. Rev.* **1995**, *95*, 987–1007. (b) Lunsford, J. H. *Catal. Today* **2000**, *63*, 165–174. (c) Olah, G. A.; Molnár, A. *Hydrocarbon Chemistry*, 2nd ed.; Wiley Interscience: Hoboken, NJ, 2003. (d) Sakakura, T.; Choi, J. C.; Yasuda, H. *Chem. Rev.* **2007**, *107*, 2365–2387. (e) Havran, V.; Duduković, M. P.; Lo, C. S. *Ind. Eng. Chem. Res.* **2011**, *50*, 7089–7100.
- (2) (a) Labinger, J. A.; Bercaw, J. E. *Nature* **2002**, *417*, 507–514. (b) Song, C. S. *Catal. Today* **2006**, *115*, 2–32. (c) Bergman, R. G. *Nature* **2007**, *446*, 391–393. (d) Copéret, C. *Chem. Rev.* **2010**, *110*, 656–680.
- (3) (a) Wang, J. G.; Liu, C. J.; Zhang, Y. P.; Eliasson, B. *Chem. Phys. Lett.* **2003**, *368*, 313–318. (b) Panjan, W.; Sirijaraensre, J.; Warakulwit, C.; Pantu, P.; Limtrakul, J. *Phys. Chem. Chem. Phys.* **2012**, *14*, 16588–16594. (c) Zhang, R. G.; Song, L. Z.; Liu, H. Y.; Wang, B. *J. Appl. Catal., A* **2012**, *443*, 50–58.
- (4) (a) Kurioka, M.; Nakata, K.; Jintoku, T.; Taniguchi, Y.; Takaki, K.; Fujiwara, Y. *Chem. Lett.* **1995**, 244. (b) Fujiwara, Y.; Taniguchi, Y.; Takaki, K.; Kurioka, M.; Jintoku, T.; Kitamura, T. *Stud. Surf. Sci. Catal.* **1997**, *107*, 275–278. (c) Taniguchi, Y.; Hayashida, T.; Kitamura, T.; Fujiwara, Y. *Stud. Surf. Sci. Catal.* **1998**, *114*, 439–442. (d) Nizova, G. V.; Suss-Fink, G.; Stanislas, S.; Shul'Pin, G. B. *Chem. Commun.* **1998**, 1885–1886. (e) Zerella, M.; Mukhopadhyay, S.; Bell, A. T. *Org. Lett.* **2003**, *5*, 3193–3196.
- (5) (a) Freund, H. J.; Wambach, J.; Seiferth, O.; Dillmann, B. *WO/1996/05163A1*, 1995. (b) Huang, W.; Xie, K. C.; Wang, J. P.; Gao, Z. H.; Yin, L. H.; Zhu, Q. M. *J. Catal.* **2001**, *201*, 100–104. (c) Wilcox, E. M.; Roberts, G. W.; Spivey, J. J. *Catal. Today* **2003**, *88*, 83–90. (d) Huang, W.; Zhang, C.; Yin, L.; Xie, K. J. *Nat. Gas Chem.* **2004**, *13*, 113–115. (e) Ding, Y. H.; Huang, W.; Wang, Y. G. *Fuel Process. Technol.* **2007**, *88*, 319–324. (f) Spivey, J. J.; Wilcox, E. M.; Roberts, G. W. *Catal. Commun.* **2008**, *9*, 685–689. (g) Sellers, H.; Spiteri, R. J.; Perrone, M. J. *Phys. Chem. C* **2009**, *113*, 2340–2346. (h) Huang, W.; Sun, W. Z.; Li, F. *AIChE J.* **2010**, *56*, 1279–1284.
- (6) Wesendrup, R.; Schwarz, H. *Angew. Chem., Int. Ed. Engl.* **1995**, *34*, 2033–2035.
- (7) (a) Liu, C. J.; Li, Y.; Zhang, Y. P.; Wang, Y.; Zou, J. J.; Eliasson, B.; Xue, B. Z. *Chem. Lett.* **2001**, 1304–1305. (b) Li, Y.; Liu, C. J.; Eliasson, B.; Wang, Y. *Energy Fuels* **2002**, *16*, 864–870. (c) Zhang, Y. P.; Li, Y.; Wang, Y.; Liu, C. J.; Eliasson, B. *Fuel Process. Technol.* **2003**, *83*, 101–109.
- (8) (a) Kazansky, V. B.; Serykh, A. I.; Pidko, E. A. *J. Catal.* **2004**, *225*, 369–373. (b) Kolyagin, Y. G.; Ivanova, I. I.; Ordonsky, V. V.; Gedeon, A.; Pirogov, Y. A. *J. Phys. Chem. C* **2008**, *112*, 20065–20069. (c) Kolyagin, Y. G.; Ivanova, I. I.; Pirogov, Y. A. *Solid State Nucl. Magn. Reson.* **2009**, *35*, 104–112. (d) Luzgin, M. V.; Rogov, V. A.; Arzumanov, S. S.; Toktarev, A. V.; Stepanov, A. G.; Parmon, V. N. *Angew. Chem., Int. Ed.* **2008**, *47*, 4559–4562. (e) Luzgin, M. V.; Rogov, V. A.; Arzumanov, S. S.; Toktarev, A. V.; Stepanov, A. G.; Parmon, V. N. *Catal. Today* **2009**, *144*, 265–272. (f) Wu, J. F.; Wang, D. W.; Xu, J.; Deng, F.; Wang, W. *Chem.—Eur. J.* **2010**, *16*, 14016–14025. (g) Wang, X. M.; Qi, G. D.; Xu, J.; Li, B. J.; Wang, C.; Deng, F. *Angew. Chem., Int. Ed.* **2012**, *51*, 3850–3853. (h) Xu, J.; Zheng, A. M.; Wang, X. M.; Qi, G. D.; Su, J. H.; Du, J. F.; Gan, Z. H.; Wu, J. F.; Wang, W.; Deng, F. *Chem. Sci.* **2012**, *3*, 2932–2940. (i) Li, L.; Li, G. D.; Yan, C.; Mu, X. Y.; Pan, X. L.; Zou, X. X.; Wang, K. X.; Chen, J. S. *Angew. Chem., Int. Ed.* **2011**, *50*, 8299–8303.
- (9) (a) Hammond, C.; Jenkins, R. L.; Dimitratos, N.; Lopez-Sanchez, J. A.; Ab Rahim, M. H.; Forde, M. M.; Thetford, A.; Murphy, D. M.; Hagen, H.; Stangland, E. E.; Moulijn, J. M.; Taylor, S. H.; Willock, D. J.; Hutchings, G. J. *Chem.—Eur. J.* **2012**, *18*, 15735–15745. (b) Hammond, C.; Forde, M. M.; Ab Rahim, M. H.; Thetford, A.; He, Q.; Jenkins, R. L.; Dimitratos, N.; Lopez-Sanchez, J. A.; Dummer, N. F.; Murphy, D. M.; Carley, A. F.; Taylor, S. H.; Willock, D. J.; Stangland, E. E.; Kang, J.; Hagen, H.; Kiely, C. J.; Hutchings, G. J. *Angew. Chem., Int. Ed.* **2012**, *51*, 5129–5133. (c) Li, L.; Cai, Y. Y.; Li, G. D.; Mu, X. Y.; Wang, K. X.; Chen, J. S. *Angew. Chem., Int. Ed.* **2012**, *51*, 4702–4706. (d) Starokon, E. V.; Parfenov, M. V.; Arzumanov, S. S.; Pirutko, L. V.; Stepanov, A. G.; Panov, G. I. *J. Catal.* **2013**, *300*, 47–54. (e) He, J.; Xu, T.; Wang, Z.; Zhang, Q.; Deng, W.; Wang, Y. *Angew. Chem., Int. Ed.* **2012**, *51*, 2438–2442. (f) Choudhary, V. R.; Kinage, A. K.; Choudhary, T. V. *Science* **1997**, *275*, 1286–1288. (g) Choudhary, V. R.; Mondal, K. C.; Mulla, S. A. R. *Angew. Chem., Int. Ed.* **2005**, *44*, 4381–4385. (h) Grootaert, M. H.; Smeets, P. J.; Sels, B. F.; Jacobs, P. A.; Schoonheydt, R. A. *J. Am. Chem. Soc.* **2005**, *127*, 1394–1395. (i) Woertink, J. S.; Smeets, P. J.; Grootaert, M. H.; Vance, M. A.; Sels, B. F.; Schoonheydt, R. A.; Solomon, E. I. *Proc. Natl. Acad. Sci. U.S.A.* **2009**, *106*, 18908–18913. (j) Smeets, P. J.; Hadt, R. G.; Woertink, J. S.; Vanelderden, P.; Schoonheydt, R. A.; Sels, B. F.; Solomon, E. I. *J. Am. Chem. Soc.* **2010**, *132*, 14736–14738. (k) Ma, D.; Shu, Y. Y.; Zhang, W. P.; Han, X. W.; Xu, Y. D.; Bao, X. H. *Angew. Chem., Int. Ed.* **2000**, *39*, 2928–2931. (l) Liu, H. M.; Bao, X. H.; Xu, Y. D. *J. Catal.* **2006**, *239*, 441–450. (m) Zheng, H.; Ma, D.; Bao, X.; Hu, J. Z.; Kwak, J. H.; Wang, Y.; Peden, C. H. F. *J. Am. Chem. Soc.* **2008**, *130*, 3722–3723.
- (10) (a) Hunger, M.; Wang, W. *Adv. Catal.* **2006**, *50*, 149–225. (b) Hunger, M. *Prog. Nucl. Magn. Reson. Spectrosc.* **2008**, *53*, 105–127. (c) Wang, W.; Hunger, M. *Acc. Chem. Res.* **2008**, *41*, 895–904. (d) Ivanova, I. I.; Kolyagin, Y. G. *Chem. Soc. Rev.* **2010**, *39*, 5018–5050. (e) Blasco, T. *Chem. Soc. Rev.* **2010**, *39*, 4685–4702. (f) Stepanov, A. G. *Kinet. Catal.* **2010**, *51*, 854–872. (g) Zhang, W.; Xu, S.; Han, X.; Bao, X. *Chem. Soc. Rev.* **2012**, *41*, 192–210. (h) Zhang, L.; Ren, Y.; Yue, B.; He, H. *Chem. Commun.* **2012**, *48*, 2370–2384.
- (11) Stepanov, A. G.; Arzumanov, S. S.; Gabrienko, A. A.; Toktarev, A. V.; Parmon, V. N.; Freude, D. *J. Catal.* **2008**, *253*, 11–21.
- (12) Lazo, N. D.; Murray, D. K.; Kieke, M. L.; Haw, J. F. *J. Am. Chem. Soc.* **1992**, *114*, 8552–8559.
- (13) Luzgin, M. V.; Rogov, V. A.; Kotsarenko, N. S.; Shmachkova, V. P.; Stepanov, A. G. *J. Phys. Chem. C* **2007**, *111*, 10624–10629.
- (14) Eberstadt, M.; Gemmecker, G.; Mierke, D. F.; Kessler, H. *Angew. Chem., Int. Ed. Engl.* **1995**, *34*, 1671–1695.

(15) (a) Boudier, A.; Bromm, L. O.; Lotz, M.; Knochel, P. *Angew. Chem., Int. Ed.* **2000**, *39*, 4414–4435. (b) Pu, L.; Yu, H. B. *Chem. Rev.* **2001**, *101*, 757–824. (c) Mulvey, R. E. *Organometallics* **2006**, *25*, 1060–1075.

(16) Ochiai, H.; Jang, M.; Hirano, K.; Yorimitsu, H.; Oshima, K. *Org. Lett.* **2008**, *10*, 2681–2683.

(17) Kobayashi, K.; Kondo, Y. *Org. Lett.* **2009**, *11*, 2035–2037.

(18) Metzger, A.; Bernhardt, S.; Manolikakes, G.; Knochel, P. *Angew. Chem., Int. Ed.* **2010**, *49*, 4665–4668.

(19) Hunger, M. *Catal. Rev.: Sci. Eng.* **1997**, *39*, 345–393.

(20) Sun, M.; Abou-Hamad, E.; Rossini, A. J.; Zhang, J.; Lesage, A.; Zhu, H.; Pelletier, J.; Emsley, L.; Caps, V.; Basset, J. M. *J. Am. Chem. Soc.* **2013**, *135*, 804–810.

(21) Shi, D.; Feng, Y.; Zhong, S. *Catal. Today* **2004**, *98*, 505–509.

(22) Jessop, P. G.; Ikariya, T.; Noyori, R. *Nature* **1994**, *368*, 231–233.

(23) (a) Jessop, P. G.; Ikariya, T.; Noyori, R. *Chem. Rev.* **1995**, *95*, 259–272. (b) Leitner, W. *Angew. Chem., Int. Ed. Engl.* **1995**, *34*, 2207–2221. (c) Jessop, P. G.; Joó, F.; Tai, C.-C. *Coord. Chem. Rev.* **2004**, *248*, 2425–2442. (d) Yu, K. M. K.; Yeung, C. M. Y.; Tsang, S. C. *J. Am. Chem. Soc.* **2007**, *129*, 6360–6361. (e) Federsel, C.; Jackstell, R.; Beller, M. *Angew. Chem., Int. Ed.* **2010**, *49*, 6254–6257. (f) Wang, W.; Wang, S.; Ma, X.; Gong, J. *Chem. Soc. Rev.* **2011**, *40*, 3703.